Published in final edited form as:
Wound Repair Regen. 2010 ; 18(5): 467–477. doi:10.1111/j.1524-475X.2010.00608.x.

Delayed Wound Healing in Diabetic (db/db) Mice with Pseudomonas aeruginosa Biofilm Challenge – A Model for the Study of Chronic Wounds

Ge Zhao, MD, PhD[1], **Phillip C. Hochwalt, MD**[1], **Marcia L. Usui, BS**[1], **Robert A. Underwood, BFA**[1], **Pradeep K. Singh, MD**[2,3], **Garth A. James, PhD**[4], **Philip S. Stewart, PhD**[4], **Philip Fleckman, MD**[1], and **John E. Olerud, MD**[1]

[1]Department of Medicine Division of Dermatology, University of Washington, Seattle, WA

[2]Department of Medicine Pulmonary and Critical Care, University of Washington, Seattle, WA

[3]Department of Microbiology, University of Washington, Seattle, WA

[4]Center for Biofilm Engineering, Montana State University, Bozeman, MT

Abstract

Chronic wounds are a major clinical problem that leads to considerable morbidity and mortality. We hypothesized that an important factor in the failure of chronic wounds to heal was the presence of microbial biofilm resistant to antibiotics and protected from host defenses. A major difficulty in studying chronic wounds is the absence of suitable animal models. The goal of this study was to create a reproducible chronic wound model in diabetic mice by application of bacterial biofilm. Six millimeter punch biopsy wounds were created on the dorsal surface of diabetic (db/db) mice, subsequently challenged with *Pseudomonas aeruginosa* (PAO1) biofilms two days post-wounding, and covered with semi-occlusive dressings for two weeks. Most of the control wounds were epithelialized by 28 days post-wounding. In contrast, none of biofilm challenged wounds were closed. Histological analysis showed extensive inflammatory cell infiltration, tissue necrosis and epidermal hyperplasia adjacent to challenged wounds- all indicators of an inflammatory non-healing wound. Quantitative cultures and transmission electron microscopy demonstrated that the majority of bacteria were in the scab above the wound bed rather than in the wound tissue. The model was reproducible, allowed localized cutaneous wound infections without high mortality and demonstrated delayed wound healing following biofilm challenge. This model may provide an approach to study the role of microbial biofilms in chronic wounds as well as the effect of specific biofilm therapy on wound healing.

Keywords

wound matrix; bacteria; scab; immunohistology; electron microscopy

INTRODUCTION

Chronic wound infection is a major clinical problem that leads to high morbidity, mortality and cost. While there is no consensus definition of chronic wounds, it is generally agreed that a human wound is classified as chronic if it remains open for longer than 6–8 weeks[1, 2]. The wounds are characterized by bacterial burden, chronic inflammation and an unbalanced

Corresponding Author: Ge Zhao, MD, PhD University of Washington - Medicine/Dermatology 1959 NE Pacific St; Box 356524 Seattle, Washington 98195 T: 206-543-1088 F: 206-543-2489 zhaoge@uw.edu.

cellular defense mechanism2. Multiple species of bacteria, including Staphylococcus aureus, Pseudomonas aeruginosa, Bacteroides spp., Peptostreptococcus, Enterococcus spp., and *Streptococcus pyogenes*, have been isolated from chronic wounds, even though the wound may not show any clinical signs of localized infection. Many other bacterial species have been identified by using advanced molecular techniques3.

Recent clinical data have shown that microbial biofilms are likely to be present in chronic wounds, and it has been proposed that biofilms are a major contributor to the development and maintenance of chronicity of wounds4. Biofilms are a structured community of microorganisms enclosed in a self-produced matrix that is adherent to both an inert or living surface5. The infections caused by biofilms are characterized by surface-associated infecting microorganism, microorganism clusters encased in an extracellular matrix, confined local infection, and resistance to antibiotic treatment6. Current topical and systemic antibiotics are minimally effective in the treatment of these microbial communities. In addition, the host's inflammatory response is ineffective in combating the presence of biofilm7.

A major difficulty in formulating new therapies for chronic wounds is the lack of a satisfactory animal model in which chronic wounds can be systematically studied. Researchers have tried several methods to induce chronic wounds, such as the ischemic rabbit ear model8, radiation impaired rats9 and diabetic mice10, 11. Studies, to date, have shown it is easier to injure the tissue than to induce a reproducible model in which the chronic wound healing response is initiated12. Wound healing in these models is usually delayed only by a very short period of time or progresses so aggressively that the infection becomes systemic and results in high mortality13, 14.

The db/db mouse has been widely used for studies associated with diabetes. The db/db mouse has a spontaneous genetic mutation of the leptin receptor in the hypothalamus and loses control of satiation. The mouse overeats and eventually resembles human type 2 diabetes mellitus, with obesity, hyperglycemia, peripheral neuropathy and delayed wound healing. In addition to the type 2 diabetes phenotype, db/db mice take approximately twice as long to heal wounds as non-diabetic heterozygous littermates under certain conditions. Wound closure in db/db mice is primarily by epidermal migration rather than wound contraction15. Much of the current research on wound healing in diabetic mice has focused on the effects of such factors as inflammatory cytokines, growth factors, neuropeptides, matrix metalloproteinases, tissue inhibitor of metalloproteinases, low oxygen, and cellular senescence16, 17. Targeting biofilms that are present on the surface of chronic wounds may be an effective strategy to promote healing of chronic wounds1. Our goal was to develop a diabetic mouse model in which we could study the role of biofilm in chronic wounds.

In this study we developed a biofilm challenged wound model in the db/db mouse by inoculating the wound with *P. aeruginosa* biofilm and maintaining unhealed wound for 28 days. This model provides a reproducible mouse wound with localized cutaneous infection while avoiding systemic infection. The model may enable investigation of specific mechanisms by which biofilms impair healing, and facilitate the screening of emerging anti-biofilm strategies on wound healing.

METHODS

Animals and wounding

Eighteen genetically diabetic female mice (db/db; BKS.Cg-Dock7^{m} +/+ Lepr^{db}/J) 11 weeks of age were purchased from Jackson Laboratory (Bar Harbor, ME) for the study described below. Three pilot studies were conducted on a total of fourteen mice to test various technical methodologies. Mice were housed individually in the University of Washington

Department of Comparative Medicine vivarium with ad libitum rodent chow and water. These studies were conducted with University of Washington Internal Animal Care and Use Committee approval in compliance with the NIH guide for the Care and Use of Laboratory Animals, 1985. The mice were anesthetized with an intraperitoneal injection of ketamine (0.132mg/g weight) and xylazine (20mg/ml) (Phoenix Pharmaceuticals, Inc., St. Joseph, MO). The dorsal skin was shaved, treated with depilatory cream to remove hair, then cleaned with povidone-iodine solution followed by an alcohol wipe. One circular, full-thickness wound was created on the dorsal skin of each mouse using a 6 mm biopsy punch. Mice were placed on a warming pad (37°C) until they fully recovered from surgery and then recaged.

P. aeruginosa biofilm

Biofilms were prepared by modifying the method developed at Center for Biofilm Engineering at Montana State University18. Six millimeter diameter polycarbonate membrane filters (0.2 μm pore size, GE, Minnetonka, MN) were cut using a 6 mm biopsy punch (Acuderm, Inc., Ft. Lauderdale, FL), and sterilized with exposure to UVC light for 5 minutes on both sides. *P. aeruginosa* (PAO1) from frozen stock was grown overnight in lysogeny broth (LB) medium at 37°C on a shaker. The PAO1 culture was diluted 1:1000 in sterile phosphate buffer solution (PBS); 2 μl of the diluted solution was placed on each of the 6 mm filters, which were plated on LB agar plates cultured at 37°C for 72 h. Filters with PAO1 were transferred to fresh LB agar plates at 24 and 48 hours. On average, PAO1 organisms amplified to levels of 1.2×10^8 colony forming units (CFU) per membrane after 24 h and 4.7×10^9 CFU per membrane after 72 h incubation.

Biofilm application and animal care

Application of biofilm on mice was performed 48 hours after the initial wounding procedure. The bacteria-inoculated filters were removed from the agar plate after 72 hours of incubation. A single filter was placed on each wound so the surface with bacterial biofilm was in direct contact with the wound. The filter was then removed from the wound, leaving behind the PAO1 biofilm. Nine mice were inoculated with biofilm and 8 control mice did not receive biofilm. Mastisol® liquid adhesive was applied to the skin surrounding the wound and allowed to dry for 2 min. Wounds were then covered with a 2 cm diameter transparent and semi-occlusive dressing (Tegaderm®, 3M, St. Paul, MN). All the dressings were removed at day 17. Mice were observed twice a week until day 28 post-wounding. To evaluate overall health of the mice, weight was monitored throughout the experiment. Mice losing more than 30% weight would be euthanized.

Wound harvesting/Serum albumin levels/Blood glucose

At day 28 after wounding, all 17 mice were euthanized with a 0.25 ml intraperitoneal injection of pentobarbital sodium (390 mg/ml) and phenytoin sodium (50 mg/ml) (Schering-Plough Animal Health, Union, NJ). After the mice were euthanized, 0.1ml blood was extracted from the hearts of 3 mice from each group, spread on LB agar plates and incubated at 37°C overnight. Serum albumin levels were measured in both control and biofilm challenged db/db mice using Mouse Albumin ELISA Kit (GenWay Biotech, Inc. 40-374-130046, San Diego, CA). After the mice were euthanized, 0.5 ml blood was extracted from the heart of all 17 mice, incubated at 4°C overnight, and centrifuged at 5,000 rpm for 10 min. The supernatants were collected and diluted 1:500,000. A 50 μl sample was used to determine albumin levels according to Kit instruction. A One Touch® Blood Glucose Meter (LifeScan Inc., Milpitas, CA) was used to measure blood glucose levels.

Each wound was removed including a 0.5 cm margin of surrounding skin, and placed in either sterile PBS for bacterial CFU counting, 10% neutral buffered formalin for paraffin

embedding (histology), half strength Karnovsky's for Polybed®-embedding for light and transmission electron microscopy, or O.C.T. (Sakura Finetek Inc., Torrance, CA) for cryosectioning and immunohistochemistry.

Wound documentation and measurements

Wound area was evaluated by macro photography. Mouse wounds and a metric ruler were photographed using a Nikon D1 digital camera equipped with a Micro Nikkor macro lens and dual electronic flash (Nikon, Tokyo, Japan). Polarizing filters were fitted over both the lens and flash. Cross-polarization of these filters is necessary to remove spectral reflections from the Tegaderm® and wound surface. The wound size was measured by image calibration using the metric ruler and subsequent calculation of wound area using image analysis (Photoshop with IP tools Plug-in, Reindeer Graphics, Asheville, NC).

Colony formation unit (CFU) counting

Three mice from each group were randomly selected to determine bacterial quantity. The scab, excised wound, and normal skin from each mouse were collected into separate tubes with 1 ml PBS. All the tissues were homogenized at 26,000rpm for 30 seconds (Polytran® PT 3100 Benchtop Large-Scale Homogenizer, Capitol Scientific Inc., Austin, TX). The resulting solutions were serially diluted and plated on LB agar and incubated overnight at 37°C. CFUs were determined by standard colony counting method.

Histology

Wound samples from 4 db/db control mice and 5 db/db biofilm challenged mice were evaluated for histologic study. Six micron paraffin and O.C.T. frozen sections were stained with hematoxylin-eosin (H&E). H&E stained tissue was evaluated for re-epithelialization, granulation tissue, and inflammatory response. Six micron sections of O.C.T. embedded tissue were Gram stained to evaluate the presence of bacteria. To determine the percentage of wound closure, the distance between two epithelial tongues in the center of the wound was divided by the distance between original wound edges. The original wound edge was determined as the point where subcutaneous fat tissue was no longer visible.

Immunohistochemistry

Six-micron sections of O.C.T.-embedded implant specimens were immunolabeled using routine immunoperoxidase methods as previously described19. Primary antibodies used were: Pankeratin (Panker) (rabbit, 1:1000, Dako, Carpenteria, CA), Keratin 14 (K14) (rabbit, 1:1000, Covance, Princeton, NJ), platelet/endothelial cell adhesion molecule-1 (PECAM-1 or CD-31) (rat, 1:400, Research Diagnostics, Concord, MA), integrin β4 (rat, 1:2000, BD Biosciences Pharmingen, San Jose, CA), P3C8 – laminin 332 (rat, 1:10, gift from Dr. William Carter), R5808 – uncleaved alpha3 chain of laminin 332 (rat, 1:1000, gift from Dr. William Carter), neurofilament 200 (rabbit, 1:1000, Sigma, St. Louis, MO), and Ki67 (rabbit, 1:1000, Abcam Inc., Cambridge, MA). Secondary antibodies used were biotinylated goat anti-rat (1:1600, Jackson ImmunoResearch, West Grove, PA) or biotinylated goat anti-rabbit (1:300, Vector Laboratories, Burlingame, CA). Following secondary antibody labeling, sections were incubated with streptavidin-biotin complex [Vectastain Elite ABC kit (peroxidase), Vector Laboratories, Burlingame, CA], with 0.12% 3,3'-diaminobenzidine used as chromogen. Glycergel (Dako, Carpenteria, CA) was used as mounting medium. Tissue sections were viewed using a Nikon Microphot-SA microscope. Images were captured using a Photometrics Sensys digital camera controlled by IP Lab software (Scanalytics, Fairfax, VA). Brightfield and differential interference contrast (DIC) images were captured to evaluate H&E and IHC stained tissues. Photoshop® (Adobe

Systems Inc., San Jose, CA) was used for image color adjustment, image analysis and figure preparation.

Transmission electron microscopy

The tissue region of interest was excised and fixed for a minimum of 24 hours in half strength Karnovsky's, then further dissected to remove excess tissue and allowed to fix for an additional 48 hours at 4°C. Tissue blocks were post-fixed in 1% osmium tetroxide, stained en bloc with 1% uranyl acetate, dehydrated through a graded ethanol series and embedded in Polybed 812® (Polysciences Inc. Warrington, PA). Semithin sections, 1μm in thickness, were stained with Richardson's stain for examination using light microscopy. Ultrathin sections 60–80nm in thickness were collected on formvar coated copper grids and stained with 1% phosphotungstic acid, 3% uranyl acetate, and lead citrate and examined using a JEOL 1200 transmission electron microscope (JEOL, Tokyo, Japan) equipped with a Megaview digital imaging system (Olympus Soft Imaging Solutions, Lakewood, Co, USA).

Data analysis

Data were analyzed using Excel 2007 (Microsoft Inc., Redmond, WA). Values were expressed as means ± standard error. Significant level was set at $\alpha=0.05$. Differences in wound sizes, albumin and glucose levels between groups were determined using general linear model ANOVA and one sided student *t*-tests.

RESULTS

Mice physical health

In pilot studies, we found that inoculation at the time of wounding led to significantly enlarged wounds, variable wound size, loss of more than 30% pre-wounding weight, and high mortality22. Therefore, we transferred the biofilm onto the wounds two days after wounding in this study. At day 0 the db/db mice ranged in weight from 36.7 to 46.3 g. Average weight of the control group was 40.8 g, and of the mice with *P. aeruginosa* (PAO1) biofilm challenged wounds (referred as PAO1 group below) was 42.0 g. One mouse from the control group did not recover from the initial wound surgery. The remaining 17 mice were healthy, showing no signs of systemic infection for the duration of the study. The average weight loss at the time of tissue harvest for the control group was 10.1±4.1% and for the PAO1 group was 14.3±2.1% (Figure 1). The difference in weight loss between the two groups was not statistically significant. To evaluate protein malnutrition due to chronic infection which may impair wound healing, serum albumin levels were measured. The average albumin level for the control group was 42.7±2.39 mg/ml and for the PAO1 group was 40.95±1.57 mg/ml. The difference in albumin levels between the two groups was not statistically significant. The blood glucose levels, another factor that may impact wound healing, were also comparable between control and PAO1 groups. The baseline glucose levels were 333±60 mg/dL in the control group and 375±26 mg/dL in the PAO1 group. At 28 days post-wounding, the blood glucose levels were >597 mg/dL and >600 mg/dL in the two groups respectively.

Wound morphology

Wounds created by 6 mm biopsy punch were consistent in size and shape without significant bleeding (Figure 2). Forty-eight hours post-wounding at the time of biofilm challenge, the wounds retained their original size, and all wound surfaces were dry without obvious signs of infection. Mastisol® adhesive glue induced slight erythema around the wounds of some mice in both control and PAO1 groups. On day 7 post-wounding (5 days after biofilm challenge), the wounds accumulated approximately 0.1 ml exudate. Exudate is “material,

such as fluid, cells or cellular debris, which has escaped from blood vessels or is produced by cells locally, and has been deposited in tissue or tissue surfaces20". Larger amounts of exudates were observed on the wounds of PAO1 group, and were yellow in color and thicker in consistency than those from control group. On day 15, one mouse in the control group and 3 mice in the PAO1 group lost their adhesive dressing. On day 17, the remaining adhesive dressings were removed, exposing the wounds to the environment. Once the dressings were removed, exudates dried and formed scabs on all the wounds. We define scab as a crust of dried blood, serum and exudate over the wound during healing. At day 28, 5 mice in the control group had lost their scabs and the wounds looked healed by gross examination. The wounds in the remaining 3 mice in the control group were still covered by scabs. All 9 wounds in the PAO1 group had intact scabs. The skin adjacent to the wounds was different between the two groups. While no control mouse had any skin color change around the wound, 5 mice of the PAO1 group showed hyperpigmentation around the wound (Figure 2l) and the other 4 mice in PAO1 group showed regenerated hair encircling the wound (data not shown).

Bacteriology

To evaluate the relationship between bacterial burden and wound healing, we quantified CFU of bacteria in scabs, wounds, and normal unaffected skin at least 2 cm away from the wound at the time of harvest. Only 3 of the 8 control wounds retained scabs at 28 days (Figure 3a). Two scabs, 3 wounds and 3 areas of unwounded skin from 3 controls were evaluated. One scab had a count of 10^7 CFU and the other scab had a CFU of 1.4×10^4. The control group wounds and unaffected skin all had counts of 10^3–10^5 CFUs. In the PAO1 group, scabs, wounds and unaffected skin were evaluated in 3 mice (Figure 3b). The scabs had counts of 2×10^7, 6.5×10^7 and 6.5×10^4 CFUs while both the wounds and unaffected skins had counts of 10^3 – 10^5. Organism identification showed that the bacteria were the combination of *P. aeruginosa* and *S. aureus* in both control and PAO1 wounds. Gram staining of 7 control wounds and 8 wounds matrices in PAO1 group failed to reveal bacteria. The scabs were too structurally loose to remain intact during the processing and staining process; however, bacteria were observed in the scabs studied by transmission electron microscopy as described below. Blood cultures from both groups were negative.

Histology

Three of the 4 control wounds we examined were fully re-epithelialized. The epidermis and dermis were significantly thicker than the adjacent normal skin, with higher cellular density (Figure 4a). One control wound, which was covered by scab, was not completely healed with wound closure of 53% of the original diameter. None of the 5 wounds in the PAO1 group we examined were healed (Figure 4b). The average closure in diameter of wounds in PAO1 group was 48±8% (Table 1). In addition to hyperplastic epidermis and thickened dermis, clusters of inflammatory cells formed microabcesses. The wounds in the PAO1 group were filled with a mixture of homogenous non-cellular debris and infiltrated neutrophils.

Immunohistochemistry

To better understand the histological change during the chronic wound healing, we performed immunohistochemistal staining to identify skin associated structures. Consistent with the H&E staining (Figure 5a–c), keratin staining showed complete re-epithelialization of control wounds, and partial re-epithelialization of wounds in the PAO1 group (Figure 5d–f). The wound epidermis was approximately 5 times thicker than adjacent normal skin. Parakeratosis (retained nuclei) was present in the stratum corneum of the PAO1 group wounds. Immunostaining using the cell proliferating Ki67 antibody, which stains

proliferative cells in the basal layer of newborn mouse skin (Figure 5g insert), showed only a few Ki67 positive cells in the basal layer of all samples (Figure 5g–i).

Examination of basement membrane markers confirmed the findings of keratin and H&E staining. The antibody to the β_4 subunit of integrin $\alpha_6\beta_4$, a plasma membrane receptor that mediates cell attachment, showed a strong linear pattern along the basement membrane, and also stained the cytoplasm in the basal cells (Figure 6a–c). Laminin 332 (formerly laminin 5) is a major matrix protein in the basement membrane and the ligand of integrin $\alpha_6\beta_4$. Cleaved laminin 332, labeled by antibody P3C8, showed a linear pattern along the basement membrane (Figure 6d–f). The R5808 antibody was used to detect the uncleaved alpha 3 chain of laminin 332, which identifies regions of migrating keratinocytes in acute wounds actively undergoing new laminin 332 deposition. Uncleaved laminin 332 staining was absent from normal skin and the completely re-epithelialized control wound as is typical for normal skin and healed wounds (data not shown). In most of the wounds in PAO1 group, the migrating epithelial tongue did not show evidence of uncleaved alpha 3 chain of laminin 332.

The dermis was also much thicker in the wounds of both control and PAO1 groups than in normal skin. The control wound was fully revascularized as indicated by PECAM staining; however, the wound matrix of the wounds in PAO1 group lacked PECAM staining (Figure 6g–i). Immunostaining with the neurofilament antibody showed no reactivity in the control wound and most of the wounds in PAO1 group (data not shown). Only one sample of wound in PAO1 group showed fragments of neurofilaments.

Transmission Electron Microscopy

Examination of multiple scabs samples from the PAO1 group showed a consistent stratification starting with a thick layer of morphologically viable appearing inflammatory cells (neutrophils) across the ventral surface of the scab (Figure 7). Above this viable neutrophil layer was a layer of non-viable neutrophils, as indicated by condensed nuclei and lack of cytoplasmic organelles, mixed with cellular and environmental debris, serum components and fibrin. The upper scab was a non-cellular amorphous matrix. Clusters of rod shaped microorganisms were observed embedded in this amorphous matrix proximal to fissures that coursed through the scab from the dorsal and lateral surfaces (Figure 8a–b). Bacteria were round or rod shape depending on the orientation of the cutting plane. An electron dense biofilm matrix surrounded the individual bacilli that was morphologically distinct from the surrounding scab matrix (Figure 8b). Small secreted vesicles were observed on the outer membrane of bacilli as well as the adjacent biofilm matrix. We observed no flagella or pili (Figure 8c). Similar clusters of bacillus as seen in the scabs were not observed within the control wounds or cutaneous wound matrix in the PAO1 group.

DISCUSSION

In this study, we developed a delayed wound healing model in diabetic mice by challenging wounds with *P. aeruginosa* biofilm as a model to study chronic wounds. This model demonstrates significant delay in wound healing compared to unchallenged control mice 28 days after wounding. These wounds are characterized by reproducible wound size, confined wound perimeter, and minimal impairment to the health of the animal. Microscopic evaluation showed persistent biofilm accumulated in the scabs, which is similar to that found in the chronic wounds of humans[4, 21]. Quantitative culture confirmed the persistence of *P. aeruginosa* infection and revealed a high density of microorganisms in the scabs.

In pilot studies, we observed that accumulation of wound exudate under the large dressing over a long period of time was the primary reason leading to uncontrolled infection and

wound expansion. The same phenomena were reported by other researchers in different models14, 23. We tested different methods to control wound spreading, including frequent changing of the dressing, absorbent dressing such as calcium alginate pad, and needle aspiration of pus. However, these methods failed because repeated changing of the dressing irritated the mouse skin or the excess purulent fluid was too viscous to be removed. During the testing, we found that the exudate that spread only slightly beyond the edge of the dressing quickly dried out and stopped expansion of the wound. Therefore, we proposed to control wound size by limiting the dressing size. The main challenge of this strategy was that the smaller the dressing, the greater the difficult in keeping the dressing in place for two weeks. Early loss of the dressings led to faster clearing of the bacteria on the dried wound and resulted in more rapid healing. After testing several methods, we selected Mastisol® liquid adhesive as the best adhesive to maximize the adherence of the applied dressing. Under these conditions most dressings remained intact for 17 days and the wound fluid was confined within the perimeter of the dressing. These changes resulted in healthier mice with well defined, non-healing wounds at day 28. It should be pointed that the delayed wound healing in this biofilm challenged wound model is different from human chronic wounds in that human chronic wounds do not require occlusive dressing for biofilm infection.

Previous studies have shown that in db/db mice the rate of re-epithelialization was 2 mm per 10 days24. Occlusive dressings splinted the wounds of db/db, and delayed the healing time of a 6 mm diameter wound from 13 to 28 days, while the wounds of their heterogeneous db/- littermates healed in 12 days, regardless of the presence of dressing15. Two reasons may contribute to delayed wound healing in db/db mice compared to wild type or db/- mice. First, similar to the mechanism of non-healing diabetic foot ulcers, hyperglycemia impairs tissue circulation and immune responses resulting in non-enzymatic glycosylation of structural and regulatory proteins. Secondly, wounds on db/db mice do not contract as much as control db/- littermates because of the obesity and distended skin of the db/db mice. The db/db mice, like humans, heal mainly through re-epithelialization. In contrast, wounds on wild type or db/- mice contract immediately after wounding, resulting in smaller wound area even at time 015. Therefore, wound healing of the biofilm challenged wounds in this model were compared to unchallenged wounds in db/db mice as a control, instead of comparison to wounds created in either wild type or db/- mice.

Compared to most of the control wounds that healed within 28 days, none of the wounds challenged with PAO1 biofilm healed by 28 days. The scabs covering these open wounds contained a high density of bacteria living in biofilm-like clusters. A study by Robson *et al.* suggested that wound healing may be impaired by bacterial load higher than 10^5 colony counts per gram of tissue25. Recent studies have revealed the relationship between surface associated biofilms and chronic wounds4–6, 26, 27. Our chronic wound model suggests there is a relationship between biofilm challenge and delayed wound healing. Weight loss, blood culture, serum albumin and blood glucose levels showed no difference between control and biofilm challenged groups, indicating differences in the wound healing process were not due to confounding systemic effects such as protein malnutrition or sepsis.

Studies of chronic ulcers in diabetic patients showed that the epidermis of ulcer margins is highly proliferative, as shown by increased Ki67 immunostaining at the margin of the ulcers and in the tissue adjacent to the ulcer margin28, 29. However, very few keratinocytes stained positively with Ki67 in the db/db chronic wound margin. For the patient population there was no control for timing of debridement which may stimulate keratinocyte proliferation. The mouse chronic wounds in our study were never debrided, thus the keratinocytes may not be stimulated to proliferate 28 days post-wounding. Intact laminin 332 is associated with active migrating keratinocytes30, and is strongly present along the margin of acute wounds, but absent in unwounded or healed skin. Its expression varies in

human diabetic chronic wounds28, which is consistent with our findings in the mouse chronic wounds. The control mouse wounds healed with vascular regeneration in the dermis, indicating granulation tissue formation during the normal wound healing process. In contrast, wounds in the PAO1 group had no vasculature in the center of the wound matrix, which is similar to human chronic wounds (data not shown). Absence of angiogenesis may also contribute to the delay of wound healing.

Biofilms resist current antibiotics and the host inflammatory response because of numerous survival strategies inherent to their community structure. Proposed biofilm survival strategies include: decreased penetration of exogenous antibiotics, failure of penetration of host generated antibodies that may bind to matrix, catalase secretion protecting against hydrogen peroxide penetration, nutrient/oxygen depletion causing growth rates below the threshold for antibiotic killing, induction of stress response genes, resistance due to prolonged antibiotic exposure, and quorum sensing31. Current antibiotic therapies target planktonic bacteria instead of biofilms. The biofilm challenge model we demonstrate will allow *in vivo* study of potential treatments specifically disrupting biofilms. In addition, treatments can be tested either systemically or topically because of the ease of access to the wound bed. New anti-biofilm treatments targeting these survival mechanisms are being studied *in vitro* and include: nitric oxide (biofilm dispersal), ribonucleic-acid-III-inhibiting peptide (quorum sensing inhibitor), gallium and lactoferrin (interferes with iron uptake and signaling in bacteria), and bioelectric effect (enhanced antimicrobial activity)32–35.

One complication of this study is the occasional contamination in the control mice. The mice were housed individually in a BSL2 level facility. Two out of 8 control mice showed signs of wound infection during the experiment period. One of these two wounds did not heal by histological analysis. The other wound was used for bacterial CFU quantification instead of histological analysis, and showed large numbers of *P. aeruginosa* and *S. aureus* in the scab. The results suggest that contamination is related to delayed wound healing, which reinforces our conclusion that the presence of biofilm contributes to chronic wound.

P. aeruginosa biofilms are more prevalent in human chronic wounds than in acute wounds4. Human ulcers infected with *P. aeruginosa* are significantly larger than those without Pseudomonas infection36. These findings support the use of *P. aeruginosa* in the study of chronic wound infection in mice. In this experiment, we grew *P. aeruginosa* using an established method of *in vitro* biofilm preparation. *P. aeruginosa* biofilms prepared in this way are significantly more resistant to the antibiotics tobramycin and ciprofloxacin than to planktonically grown cells37. Transferring biofilms from polycarbonate membrane filters to the wounds of animals is a simple and effective method of inoculating wounds. In addition, transferring preformed biofilms to wounds may enable bacterial communities with a biofilm phenotype to quickly develop an antibiotic resistant wound infection while minimizing the invasive effects of planktonically grown cells.

A major finding of this study is that more than 99% of bacteria were localized in the scab rather than directly growing on wound surface. Kennedy *et al.* also found that in human burn wounds, bacteria were not detected on structurally intact wounds; instead, they only presented on ulcerated wounds and in the eschars21. This result may explain the frequent negative culture results in clinical chronic wounds. Sharp debridement is a common procedure in chronic wound management, and is thought to convert chronic wounds into acute wounds by removing scabs and debris. Our study indicates that debridement also plays an important role in removing the bioburden and providing a healthier environment for epithelial growth. Similar to biofilm distribution on chronic wounds, in patients with cystic fibrosis, *P. aeruginosa* biofilms were identified in luminal sputum without invasion into underlying airway epithelium38. Our transmission electron microscopic images showed that

P. aeruginosa in scabs may have lost flagella and pili, and were encased in a specific extracellular matrix that was different from the surrounding scab matrix. The result is consistent with previous studies showing that the isolates from chronically infected patients or microorganisms in *in vitro* biofilms lose these appendages and mobility39. The bacterial density in cystic fibrosis patients can reach as high as 10^8 to 10^{10} CFU/ml for decades without invasive dissemination to the lung. Recent studies have shown that bacterial soluble factors delayed epithelial closure in a keratinocyte scratch wound model where *S. aureus* was separated from the keratinocytes by a Millipore filter with pores too small for the bacteria to directly contact the keratinocytes40. Our results suggest that soluble factors released from the bacteria in the biofilm may play a role in retarding wound closure.

Our data show that biofilm challenge of diabetic mouse wounds with *P. aeruginosa* provides an excellent model for studying the role of biofilm in wound healing. Wound healing is significantly impaired while animals survive for at least four weeks. This model will enable investigation of specific mechanisms by which biofilm impairs healing, facilitate the screening of numerous emerging anti-biofilm technologies and their impact on wound healing, and aid in evaluation of chronic wound care strategies. Evaluating the role of microbial biofilm in chronic wounds and developing effective anti-biofilm treatments to accelerate wound healing may have significant impact on more rapid closure of chronic wounds. Studies have been initiated to examine the antibiotic resistance of the biofilm in the scab, the natural time course of healing in this model, and the application of this method in wild type or heterogeneous mice as well as extending studies to *S. aureus* biofilm and polymicrobial biofilms.

Acknowledgments

This study was funded by National Institute of Health Grant P20 GM078445. Dr. Pradeep K. Singh was supported by grants from NIH, the Cystic Fibrosis Foundation, and the Burroughs Wellcome Fund. We appreciate the technical support provided by Elizabeth Bauerle for biofilm development and analysis, and generous donation of antibodies from Dr. William Carter.

REFERENCES

1. Fonder MA, Lazarus GS, Cowan DA, Aronson-Cook B, Kohli AR, Mamelak AJ. Treating the chronic wound: A practical approach to the care of nonhealing wounds and wound care dressings. J Am Acad Dermatol. 2008; 58:185–206. [PubMed: 18222318]
2. Tomic-Canic, M.; Agren, MS.; Alvares, OM. Epidermal Repair and Chronic Wounds. In: Rovie, DT.; Maibach, H., editors. The Epidermis in Wound Healing. CRS Press; New York: 2004. p. 26
3. Dowd SE, Sun Y, Secor PR, Rhoads DD, Wolcott BM, James GA, Wolcott RD. Survey of bacterial diversity in chronic wounds using pyrosequencing, DGGE, and full ribosome shotgun sequencing. BMC Microbiol. 2008; 8:43. [PubMed: 18325110]
4. James GA, Swogger E, Wolcott R, Pulcini E, Secor P, Sestrich J, Costerton JW, Stewart PS. Biofilms in chronic wounds. Wound Repair Regen. 2008; 16:37–44. [PubMed: 18086294]
5. Costerton JW, Stewart PS, Greenberg EP. Bacterial biofilms: a common cause of persistent infections. Science. 1999; 284:1318–22. [PubMed: 10334980]
6. Parsek MR, Singh PK. Bacterial biofilms: an emerging link to disease pathogenesis. Annu Rev Microbiol. 2003; 57:677–701. [PubMed: 14527295]
7. Kelly NM, Kluftinger JL, Pasloske BL, Paranchych W, Hancock RE. Pseudomonas aeruginosa pili as ligands for nonopsonic phagocytosis by fibronectin-stimulated macrophages. Infect Immun. 1989; 57:3841–5. [PubMed: 2572562]
8. Ahn ST, Mustoe TA. Effects of ischemia on ulcer wound healing: a new model in the rabbit ear. Ann Plast Surg. 1990; 24:17–23. [PubMed: 2301878]

9. Gu Q, Wang D, Gao Y, Zhou J, Peng R, Cui Y, Xia G, Qing Q, Yang H, Liu J, Zhao M. Expression of MMP1 in surgical and radiation-impaired wound healing and its effects on the healing process. J Environ Pathol Toxicol Oncol. 2002; 21:71–8. [PubMed: 11934016]
10. Greenhalgh DG, Sprugel KH, Murray MJ, Ross R. PDGF and FGF stimulate wound healing in the genetically diabetic mouse. Am J Pathol. 1990; 136:1235–46. [PubMed: 2356856]
11. Gibran NS, Jang YC, Isik FF, Greenhalgh DG, Muffley LA, Underwood RA, Usui ML, Larsen J, Smith DG, Bunnett N, Ansel JC, Olerud JE. Diminished neuropeptide levels contribute to the impaired cutaneous healing response associated with diabetes mellitus. J Surg Res. 2002; 108:122–8. [PubMed: 12443724]
12. Davidson JM. Animal models for wound repair. Arch Dermatol Res. 1998; 290(Suppl):S1–11. [PubMed: 9710378]
13. Davis SC, Ricotti C, Cazzaniga A, Welsh E, Eaglstein WH, Mertz PM. Microscopic and physiologic evidence for biofilm-associated wound colonization in vivo. Wound Repair Regen. 2008; 16:23–9. [PubMed: 18211576]
14. Brown RL, Greenhalgh DG. Mouse models to study wound closure and topical treatment of infected wounds in healing-impaired and normal healing hosts. Wound Repair Regen. 1997; 5:198–204. [PubMed: 16984431]
15. Sullivan SR, Underwood RA, Gibran NS, Sigle RO, Usui ML, Carter WG, Olerud JE. Validation of a model for the study of multiple wounds in the diabetic mouse (db/db). Plast Reconstr Surg. 2004; 113:953–60. [PubMed: 15108888]
16. Brem H, Tomic-Canic M. Cellular and molecular basis of wound healing in diabetes. J Clin Invest. 2007; 117:1219–22. [PubMed: 17476353]
17. Terasaki K, Kanzaki T, Aoki T, Iwata K, Saiki I. Effects of recombinant human tissue inhibitor of metalloproteinases-2 (rh-TIMP-2) on migration of epidermal keratinocytes in vitro and wound healing in vivo. J Dermatol. 2003; 30:165–72. [PubMed: 12692351]
18. Anderl JN, Franklin MJ, Stewart PS. Role of antibiotic penetration limitation in Klebsiella pneumoniae biofilm resistance to ampicillin and ciprofloxacin. Antimicrob Agents Chemother. 2000; 44:1818–24. [PubMed: 10858336]
19. Fukano Y, Knowles NG, Usui ML, Underwood RA, Hauch KD, Marshall AJ, Ratner BD, Giachelli C, Carter WG, Fleckman P, Olerud JE. Characterization of an in vitro model for evaluating the interface between skin and percutaneous biomaterials. Wound Repair Regen. 2006; 14:484–91. [PubMed: 16939578]
20. Dorland's illustrated medical dictionary. Saunders; Philadelphia, PA: 2007.
21. Kennedy P, Brammah S, Wills E. Burns, biofilm and a new appraisal of burn wound sepsis. Burns. 2010; 36:49–56. [PubMed: 19523770]
22. Hochwalt, P.; Zhao, G.; Underwood, RA.; Usui, ML.; Singh, PK.; Stewart, PS.; Olerud, JE.; Fleckman, P. International Investigative Dermatology. Kyoto, Japan: 2008. Development of a chronic wound in a diabetic (db/db) mouse by infection with biofilm.
23. Shi CM, Nakao H, Yamazaki M, Tsuboi R, Ogawa H. Mixture of sugar and povidone-iodine stimulates healing of MRSA-infected skin ulcers on db/db mice. Arch Dermatol Res. 2007; 299:449–56. [PubMed: 17680256]
24. Senter LH, Legrand EK, Laemmerhirt KE, Kiorpes TC. Assessment of full-thickness wounds in the genetically diabetic mouse for suitability as a wound healing model. Wound Repair Regen. 1995; 3:351–8. [PubMed: 17173562]
25. Robson MC, Stenberg BD, Heggers JP. Wound healing alterations caused by infection. Clin Plast Surg. 1990; 17:485–92. [PubMed: 2199139]
26. Donlan RM, Costerton JW. Biofilms: survival mechanisms of clinically relevant microorganisms. Clin Microbiol Rev. 2002; 15:167–93. [PubMed: 11932229]
27. Hall-Stoodley L, Stoodley P. Evolving concepts in biofilm infections. Cell Microbiol. 2009; 11:1034–43. [PubMed: 19374653]
28. Usui ML, Mansbridge JN, Carter WG, Fujita M, Olerud JE. Keratinocyte migration, proliferation, and differentiation in chronic ulcers from patients with diabetes and normal wounds. J Histochem Cytochem. 2008; 56:687–96. [PubMed: 18413645]

29. Andriessen MP, van Bergen BH, Spruijt KI, Go IH, Schalkwijk J, van de Kerkhof PC. Epidermal proliferation is not impaired in chronic venous ulcers. Acta Derm Venereol. 1995; 75:459–62. [PubMed: 8651025]
30. Ryan MC, Lee K, Miyashita Y, Carter WG. Targeted disruption of the LAMA3 gene in mice reveals abnormalities in survival and late stage differentiation of epithelial cells. J Cell Biol. 1999; 145:1309–23. [PubMed: 10366601]
31. Fux CA, Costerton JW, Stewart PS, Stoodley P. Survival strategies of infectious biofilms. Trends Microbiol. 2005; 13:34–40. [PubMed: 15639630]
32. Kaneko Y, Thoendel M, Olakanmi O, Britigan BE, Singh PK. The transition metal gallium disrupts Pseudomonas aeruginosa iron metabolism and has antimicrobial and antibiofilm activity. J Clin Invest. 2007; 117:877–88. [PubMed: 17364024]
33. Giacometti A, Cirioni O, Gov Y, Ghiselli R, Del Prete MS, Mocchegiani F, Saba V, Orlando F, Scalise G, Balaban N, Dell'Acqua G. RNA III inhibiting peptide inhibits in vivo biofilm formation by drug-resistant Staphylococcus aureus. Antimicrob Agents Chemother. 2003; 47:1979–83. [PubMed: 12760879]
34. Stewart PS, Wattanakaroon W, Goodrum L, Fortun SM, McLeod BR. Electrolytic generation of oxygen partially explains electrical enhancement of tobramycin efficacy against Pseudomonas aeruginosa biofilm. Antimicrob Agents Chemother. 1999; 43:292–6. [PubMed: 9925521]
35. Barraud N, Hassett DJ, Hwang SH, Rice SA, Kjelleberg S, Webb JS. Involvement of nitric oxide in biofilm dispersal of Pseudomonas aeruginosa. J Bacteriol. 2006; 188:7344–53. [PubMed: 17050922]
36. Gjodsbol K, Christensen JJ, Karlsmark T, Jorgensen B, Klein BM, Krogfelt KA. Multiple bacterial species reside in chronic wounds: a longitudinal study. Int Wound J. 2006; 3:225–31. [PubMed: 16984578]
37. Walters MC 3rd, Roe F, Bugnicourt A, Franklin MJ, Stewart PS. Contributions of antibiotic penetration, oxygen limitation, and low metabolic activity to tolerance of Pseudomonas aeruginosa biofilms to ciprofloxacin and tobramycin. Antimicrob Agents Chemother. 2003; 47:317–23. [PubMed: 12499208]
38. Baltimore RS, Christie CD, Smith GJ. Immunohistopathologic localization of Pseudomonas aeruginosa in lungs from patients with cystic fibrosis. Implications for the pathogenesis of progressive lung deterioration. Am Rev Respir Dis. 1989; 140:1650–61. [PubMed: 2513765]
39. Whiteley M, Bangera MG, Bumgarner RE, Parsek MR, Teitzel GM, Lory S, Greenberg EP. Gene expression in Pseudomonas aeruginosa biofilms. Nature. 2001; 413:860–4. [PubMed: 11677611]
40. Kirker KR, Secor PR, James GA, Fleckman P, Olerud JE, Stewart PS. Loss of viability and induction of apoptosis in human keratinocytes exposed to Staphylococcus aureus biofilms in vitro. Wound Repair Regen. 2009; 17:690–9. [PubMed: 19671124]

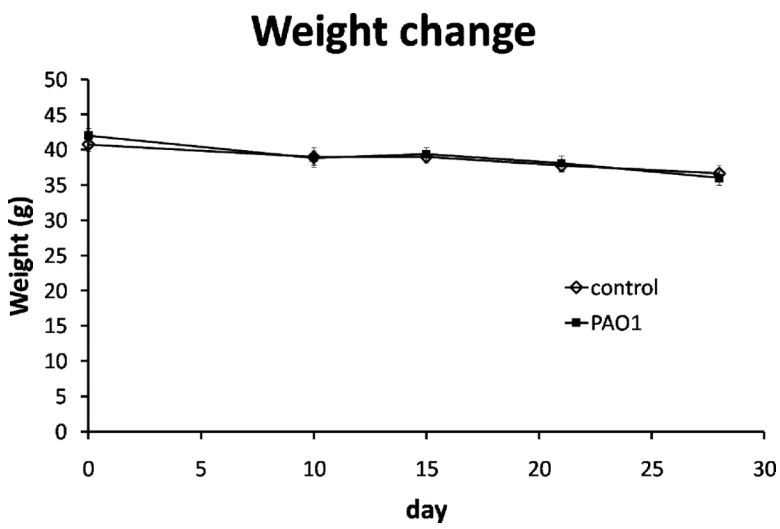

Figure 1.
Weight changes in control (◊, n=8) and PAO1 (■, n=9) groups at 0, 10, 15, 21 and 28 days post-wounding. Data are presented as mean±SD.

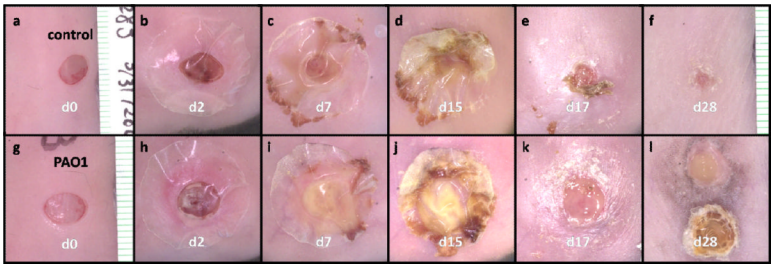

Figure 2.
Macro photographs of wounds from one selected mouse in control group (a–f) and PAO1 group (g–l) each at 0, 2, 7, 15, 17 and 28 days post-wounding. In (l), the scab was removed and inverted next to wound bed to show the interior surface of the scab.

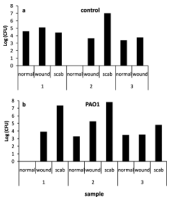

Figure 3.
CFU of normal skin, wound and scab samples in 3 control mice (a) and 3 PAO1 group mice (b) at 28 days post-wounding. One of the control mice did not have scab.

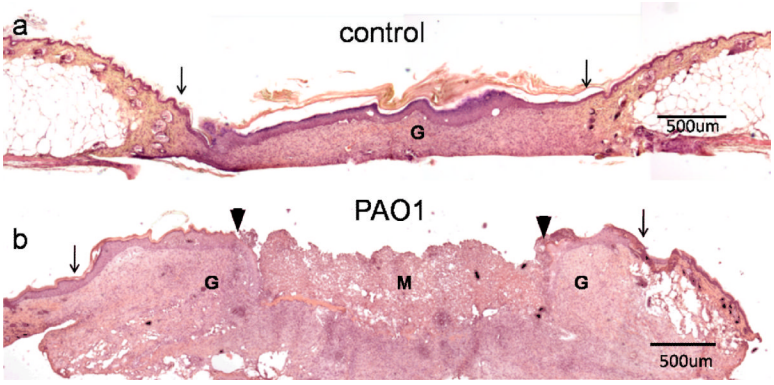

Figure 4.

H&E staining of 28 day wounds in control (a) and PAO1 group (b) mice. Original wound edge (arrow), migrating epithelial tongue (arrow head), granulation tissue (G) and wound matrix (M) are labeled.

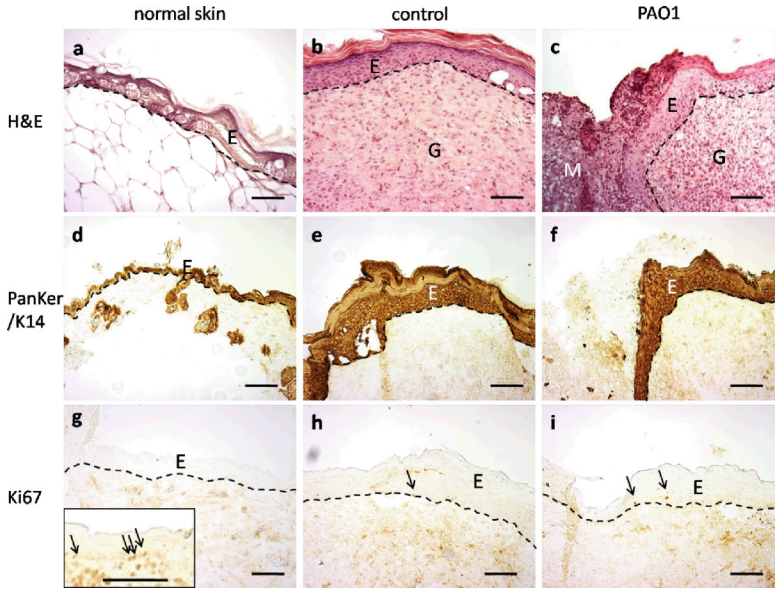

Figure 5.

H&E staining (a–c) and immunohistochemistry staining of Pankeratin/K14 (d–f) and Ki67 (g–i) in normal unaffected skin away from the wounds (a, d, g), control wounds in the central region of the wounds (b, e, h), or wound migrating tongue in PAO1 group (c, f, i). Positive control of Ki67 in newborn mice was shown in the insert in g. Arrows indicate Ki67 positive cells. Epidermal (E)-dermal junctions are outlined by dashed lines. Granulation tissue (G) and wound matrix (M) are labeled. Scale bar = 100μm.

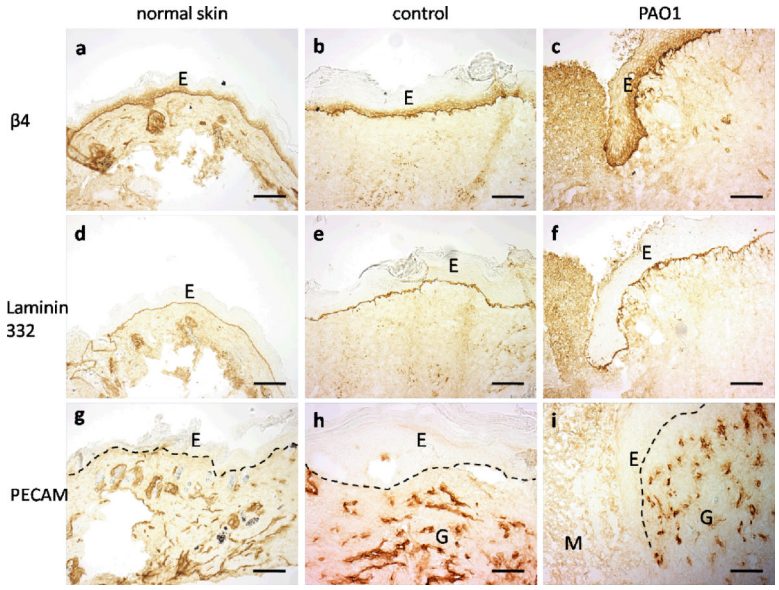

Figure 6.
Immunohistochemistry staining of integrin β4 (a–c), cleaved laminin 332 (d–f, labeled by antibody P3C8) and PECAM-1 (g–i) in normal unwounded skin away from the wounds (a, d, g), control wounds in the central region of the wounds (b, e, h) or wound migrating tongue in PAO1 group (c, f, i). Epidermal (E)-dermal junctions are outlined by dashed lines. Granulation tissue (G) and wound matrix (M) are labeled. Scale bar = 100μm.

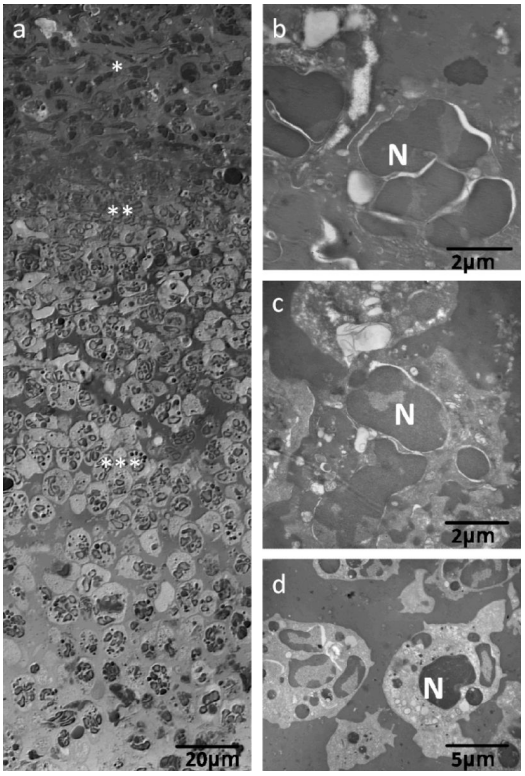

Figure 7.

Light (a) and transmission electron microscopy (b–d) images of neutrophils in the scabs. (a) Layers of neutrophils in the scabs. (b) Morphology of neutrophils (N) in the outside layer of scab (* in panel a). (c) Morphology of neutrophils (N) in the middle layer of scab (** in panel a). (d) Morphology of neutrophils (N) in the inside layer of scab (*** in panel a).

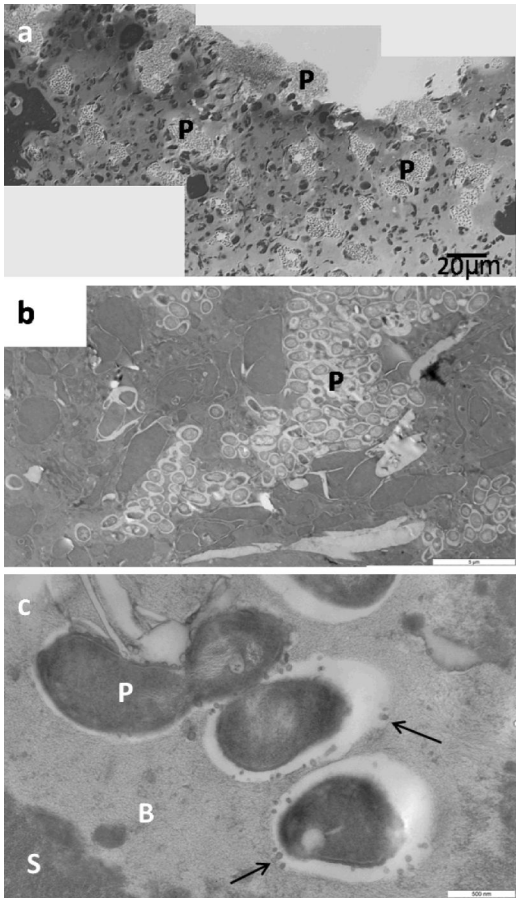

Figure 8.
Light (a) and transmission electron microscopy (b–c) images of biofilms in the scabs. (a) Light microscopy of biofilm in the scab. (b) Biofilm formed of rod shape *P. aeruginosa* (P) embedded in extracellular matrix. (c) Bacteria with vesicles (arrow). Biofilm matrix (B) shows different electron densities from scab matrix (S).

Table 1

The percentage of wound closure in length of every sample examined by histology.

Group	% of closure in length	average % of closure
control	100	88.5±11%
	100	
	100	
	53*	
PAO1	64	48±8%
	35	
	26	
	64	
	48	

* This control wound was covered by a thick scab from which *P. aeruginosa* and *S. aureus* were recovered.